JOURNAL OF THE ROYAL SOCIETY Interface

J. R. Soc. Interface (2011) **8**, 1622–1634
doi:10.1098/rsif.2011.0009
Published online 27 April 2011

Novel use of biodegradable casein conduits for guided peripheral nerve regeneration

Shih-Wei Hsiang[1], Chin-Chuan Tsai[2,3], Fuu-Jen Tsai[1], Tin-Yun Ho[1,†], Chun-Hsu Yao[1,4,†] and Yueh-Sheng Chen[1,4,*,†]

[1]*Laboratory of Biomaterials, School of Chinese Medicine, China Medical University, Taichung, Taiwan, Republic of China*
[2]*School of Chinese Medicine for Post-Baccalaureate, I-Shou University, Kaohsiung, Taiwan, Republic of China*
[3]*Department of Chinese Medicine, E-Da Hospital, Kaohsiung, Taiwan, Republic of China*
[4]*Department of Biomedical Imaging and Radiological Science, China Medical University, Taichung, Taiwan, Republic of China*

Recent advances in nerve repair technology have focused on finding more biocompatible, non-toxic materials to imitate natural peripheral nerve components. In this study, casein protein cross-linked with naturally occurring genipin (genipin-cross-linked casein (GCC)) was used for the first time to make a biodegradable conduit for peripheral nerve repair. The GCC conduit was dark blue in appearance with a concentric and round lumen. Water uptake, contact angle and mechanical tests indicated that the conduit had a high stability in water and did not collapse and cramped with a sufficiently high level of mechanical properties. Cytotoxic testing and terminal deoxynucleotidyl transferase dUTP nick-end labelling assay showed that the GCC was non-toxic and non-apoptotic, which could maintain the survival and outgrowth of Schwann cells. Non-invasive real-time nuclear factor-κB bioluminescence imaging accompanied by histochemical assessment showed that the GCC was highly biocompatible after subcutaneous implantation in transgenic mice. Effectiveness of the GCC conduit as a guidance channel was examined as it was used to repair a 10 mm gap in the rat sciatic nerve. Electrophysiology, labelling of calcitonin gene-related peptide in the lumbar spinal cord, and histology analysis all showed a rapid morphological and functional recovery for the disrupted nerves. Therefore, we conclude that the GCC can offer great nerve regeneration characteristics and can be a promising material for the successful repair of peripheral nerve defects.

Keywords: casein; nerve conduit; nerve regeneration; nerve injury

1. INTRODUCTION

For improving peripheral nerve regeneration, the development of new biodegradable materials to make nerve conduits has attracted considerable attention in recent years. In particular, such materials as polypyrrole [1], polylactic acid (PLA) [2–4] and polyglycolic acid (PGA) [5–7] are of special interest because of their soft tissue biocompatibility and the easy control of their physical and chemical properties of the polymer network. Recent advances in nerve conduit technology have focused on finding more biocompatible, non-toxic natural materials to imitate natural peripheral nerve components [8], such as collagen [9–11], gelatine [12–14] and chitosan [15–18]. In this work, our group developed a novel protein-based biodegradable conduit for nerve repair. For this purpose, casein, a predominant phosphoprotein accounting for nearly 80 per cent of proteins in cow milk [19,20] was cross-linked by genipin, which is a naturally occurring and low-cytotoxic cross-linking agent that can be obtained from its parent compound geniposide isolated from the fruits of *Gardenia jasminoides* ELLIS [21–23].

In order to understand physical characteristics of the genipin-cross-linked casein (GCC) conduits, we evaluated their mechanical function, water uptake ratio and hydrophilicity. Cytotoxic testing and terminal deoxynucleotidyl transferase dUTP nick-end labelling (TUNEL) of the conduits were determined by using the Schwann cell line, which has been extensively adopted to study cell differentiation and neurite outgrowth [24–26], to study its neuronal characteristics upon exposure to the substances released from soaked GCC conduits. Nuclear factor-κB (NF-κB)-dependent luminescent signal in transgenic mice carrying the luciferase genes accompanied by histochemical assessment were used as the guide to assess the host–GCC interaction. Finally, the effectiveness of GCC conduits as a

*Author for correspondence (yuehsc@mail.cmu.edu.tw).
†These authors contributed equally to the study.

Received 10 January 2011
Accepted 8 April 2011

guidance channel was evaluated by examining calcitonin gene-related peptide (CGRP) in the lumbar spinal cord by immunohistochemistry, and correlating morphometric and electrophysiological data after sciatic nerve transaction combined with subsequent neurorrhaphy in adult rats.

2. METHODS

2.1. Fabrication of GCC conduits

A 23 per cent (w/w) solution of casein (Sigma #C5890, Saint Louis, MO, USA) in 0.2 M Na_2HPO_4 buffer was mixed with 1.5 per cent (w/w) solution of genipin (Challenge Bioproducts Co., Taichung, Taiwan, Republic of China) at 60°C by magnetic stirring. A silicone rubber tube (1.96 mm OD; Helix Medical, Inc., Carpinteria, CA, USA) was used as a mandrel vertically dipped into the GCC solution at a constant speed where it remained for 30 s. The mandrel was then withdrawn slowly and allowed to stand for 30 s. The mandrel was rotated horizontally consistently to reduce variations in the wall thickness along the axis of the tube. Nine coating steps were used to obtain a GCC conduit with a wall thickness of about 280 μm. The coated mandrel was air-dried for one week and the GCC conduits were slipped off the silicone rubber mandrel and cut to 15 mm length. To allow fixation of the nerve tissue to the conduit, two small holes were drilled at both ends of the GCC conduits. Finally, the GCC conduits were sterilized with 25 kGy of γ-ray for subsequent implantation.

2.2. Cross-linking degree of GCC conduits

Ninhydrin assay was used to evaluate the cross-linking degree of GCC conduits. Ninhydrin (2,2-dihydroxy-1, 3-indanedione) was used to determine the amount of amino groups of each test sample. The test GCC conduits were heated with a ninhydrin solution for 20 min. After heating with ninhydrin, the optical absorbance of the solution was recorded using a spectrophotometer (Model Genesys 10, Spectronic Unicam, New York, NY, USA) at 570 nm (wavelength of the blue–purple colour) using casein at various known concentrations as standard. The amount of free amino groups in the residual casein, after heating with ninhydrin, is proportional to the optical absorbance of the solution. The cross-linking degree of GCC conduits was then determined.

2.3. Macroscopic observation of GCC conduits

To examine the morphology of the GCC explants with scanning electron microscopy (SEM), the samples were gold-coated using a Hitachi E-1010 ion sputter and micrographs were obtained using a Hitachi S3000N SEM at an accelerating voltage of 5 kV.

2.4. Mechanical function of GCC samples

The mechanical properties of GCC were determined in a dry condition. All test samples were preconditioned at 50 per cent humidity and 23°C for 48 h. The maximum tensile force was determined by the universal testing machines (AG-IS, Shimadzu Co., Japan). All test samples, cut into dumb-bell shape (figure 1), were pulled at an extension rate of 0.6 mm min^{-1}. Measurements were made five times for each sample and averages were reported.

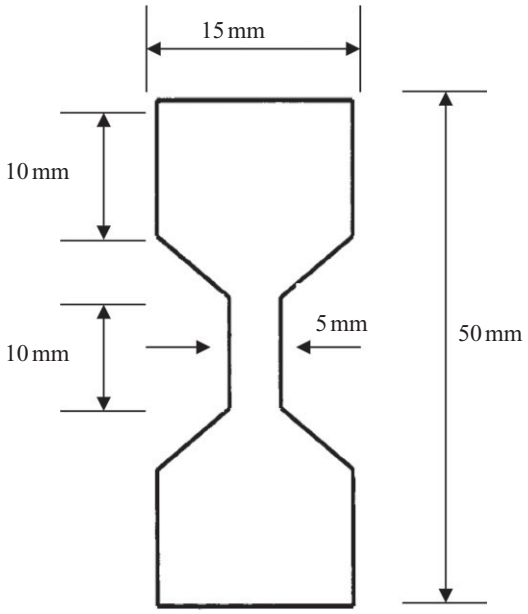

Figure 1. Schematic drawing of the dumbbell-shaped sample used in the mechanical testing (not drawn to scale).

2.5. Water contact angle analysis of GCC samples

Drops of distilled water were placed on the GCC films and contact angles were measured using a static contact angle metre (CA-D, Kyowa, Japan). An autopipette was employed with the metre to ensure that the volume of the distilled water droplet was the same (20 μl) for each specimen.

2.6. Water uptake ratio of GCC conduits

The weight equilibrium water uptake ratio was experimentally determined using the following equation:

$$\text{water uptake ratio} = \frac{\text{Wt} - W_0}{W_0},$$

where Wt is the weight of the swollen test sample and W_0 is the weight of the dried test sample. The measuring of water uptake ratio in each step is carefully conducted six times at 0.5, 1, 3, 6, 12, 24, 48, 60, 72 and 84 h after the GCC conduits were soaked in 10 ml of de-ionized water of pH 7.4 at room temperature.

2.7. Cytotoxicity and apoptosis of soaking solution of GCC conduits

The indirect cytotoxicity was conducted using an adaptation of the ISO10993-12 standard test method. GCC conduits of 6 cm^2 were washed twice with sterilized 1× phosphate-buffered saline (PBS) and dried in a laminar flow. GCC extraction solution was prepared by incubating

the conduit in 1 ml of Dulbecco's modified Eagle's Medium–serum-free medium at 37°C for 24 h in an incubator with 75 per cent humidity containing 5 per cent CO_2. RSC96 Schwann cells were seeded at 1×10^4 cells per well in a 96-well tissue-culture polystyrene plate (Corning, USA) at 37°C for 24 h in an incubator with 75 per cent humidity containing 5 per cent CO_2. After that, the culture medium was removed and replaced with the GCC extraction solution (200 µl per well). After 24 and 48 h of cell incubation with the GCC extraction solution, the solution was removed, replaced with 110 µl per well of 5 mg ml^{-1} of MTT solution in 1× PBS and further incubated in an incubator at 37°C for 4 h. Then, the MTT (3-(4,5-Dimethylthiazol-2-yl)-2,5-diphenyltetrazolium bromide) solution was removed and replaced with 50 µl of dimethyl sulphoxide to dissolve the formazan. The colour intensity was measured using a microplate reader (ELx800TM, Bio-Tek Instrument, Inc., Winoski, VT, USA) at an absorbance of 550 nm. Data were then expressed as a per cent of control level of the optical density within an individual experiment.

Apoptotic cell death was also confirmed in the present study. After treating with the GCC extraction solution for 48 h, the Schwann cells were washed with PBS twice, fixed in 2 per cent paraformaldehyde for 30 min and then permeabilized with 0.1 per cent Triton X-100/PBS for 30 min at room temperature. After washing with PBS, TUNEL assay was performed according to the manufacturer's instructions (Boehringer Mannheim). Cells were incubated in TUNEL reaction buffer in a 37°C humidified chamber for 1 h in the dark, then rinsed twice with PBS and incubated with DAPI (4′,6-diamidino-2-phenylindole) (1 mg ml^{-1}) at 37°C for 10 min, stained cells were visualized using a fluorescence microscope (Olympus DP70/U-RFLT50, Olympus Optical Co., Ltd., Japan). TUNEL-positive cells were counted as apoptotic cells.

2.8. Biocompatibility of GCC conduits

Prior to the beginning of the *in vivo* testing, the protocol was approved by the ethical committee for animal experiments of the China Medical University, Taichung, Taiwan. Transgenic mice, carrying the luciferase gene driven by NF-κB-responsive elements, were constructed as described previously [27,28]. All transgenic mice were crossed with wild-type F1 mice to yield NF-κB-luc heterozygous mice with the FVB genetic background. For insertion of the GCC implant, transgenic mice were anaesthetized with 0.12 g ketamine kg^{-1} body weight and one incision (3 mm in length) was made on the back. The GCC conduit was then implanted subcutaneously into the incision and the skin was closed with silk sutures. Six transgenic mice were randomly divided into two groups of three mice: (i) sham, the incision was made and nothing was implanted and (ii) GCC, the incision was made and the GCC conduit was implanted. The mice were imaged for luciferase activity at various time points: 1, 3, 7 and 28 days, and subsequently sacrificed for histochemical staining. For *in vivo* imaging, mice were anaesthetized with isoflurane and injected intraperitoneally with 150 mg luciferin kg^{-1} body weight. After 5 min, mice were placed facing down in the chamber and imaged for 5 min with the camera set at the highest sensitivity by IVIS Imaging System 200 Series (Xenogen, Hopkinton, MA, USA). Photons emitted from tissues were quantified using Living Image software (Xenogen). Signal intensity was quantified as the sum of all detected photon counts per second within the region of interest after subtracting the background luminescence and presented as photons s^{-1} cm^{-2} steradian^{-1} (photons s^{-1} cm^{-2} sr^{-1}). For histochemical staining, the GCC implants were retrieved and fixed in 10 per cent formalin for 2 days. Tissue was rinsed in saline and dehydrated in a series of graded alcohols (50%, 70% and 95%) for 30 min each. Samples were then embedded in paraffin and cut into thin 12 µm sections. For histomorphometric evaluation, sections were stained with haematoxylin and eosin. The tissue reactions to the implants in the subcutaneous tissue were evaluated for uniformity and thickness of the foreign body capsule as well as the inflammation responses under optical microscopy (Olympus IX70, Olympus Optical Co., Ltd).

2.9. GCC conduits implantation

Thirty adult Sprague–Dawley rats underwent placement of GCC conduits, which were removed upon sacrifice at various time points: two, five and eight weeks. Ten rats were operated at each implantation time. The animals were anaesthetized using an inhalational anaesthetic technique (AErrane, Baxter, USA). Following the skin incision, fascia and muscle groups were separated using blunt dissection, and the right sciatic nerve was severed into proximal and distal segments. The proximal stump was then secured with a single 9-0 nylon suture through the epineurium and the outer wall of the GCC conduits. The distal stump was secured similarly into the other end of the chamber. Both the proximal and distal stumps were secured to a depth of 2.5 mm into the chamber, leaving a 10-mm gap between the stumps. The muscle layer was re-approximated with 4-0 chromic gut sutures, and the skin was closed with 2-0 silk sutures. All animals were housed in temperature (22°C) and humidity (45%) controlled rooms with 12 h light cycles, and they had access to food and water ad libitum.

2.10. Electrophysiological techniques

All the animals with apparent nerve regeneration were re-anaesthetized and the sciatic nerve exposed. The stimulating cathode was a stainless-steel monopolar needle, which was placed directly on the sciatic nerve trunk, 5 mm proximal to the transection site. The anode was another stainless-steel monopolar needle placed 3 mm proximally to the cathode. Amplitude, latency and nerve conductive velocity (NCV) of the evoked muscle action potentials (MAPs) were recorded from gastrocnemius muscles with micro-needle electrodes linked to a computer system (Biopac Systems, Inc., USA). Latency was measured from stimulus to the takeoff of the first negative deflection and the amplitude from the baseline to the maximal negative peak. The NCV was carried out by placing the recording electrodes in the gastrocnemius muscles and stimulating the sciatic nerve proximally and distally to the nerve conduit and

calculated by dividing the distance between the stimulating sites by the difference in latency time.

2.11. Histological processing

Immediately after the recording of MAP, all the rats were perfused transcardially with 150 ml of normal saline followed by 300 ml of 4 per cent paraformaldehyde in 0.1 M phosphate buffer, pH 7.4. After perfusion, the L4 spinal cord was quickly removed and post-fixed in the same fixative for 3–4 h. Tissue samples were placed overnight in 30 per cent sucrose for cryoprotection at 4°C, followed by embedding in optimal cutting temperature solution. Samples were then kept at −20°C until preparation of 18 μm sections was performed using a cryostat, with samples placed upon poly-L-lysine-coated slide. Immunohistochemistry of frozen sections was carried out using a two-step protocol according to the manufacturer's instructions (Novolink Polymer Detection System, Novocastra, UK). Briefly, frozen sections were required endogenous peroxidase activity was blocked with incubation of the slides in 0.3 per cent H_2O_2, and non-specific binding sites were blocked with Protein Block (RE7102; Novocastra). After serial incubation with rabbit-anti-CGRP polyclonal antibody 1 : 1000 (Calbiochem, Germany), Post Primary Block (RE7111; Novocastra) and secondary antibody (Novolink Polymer RE7112), the sections were developed in diaminobenzidine solution under a microscope and counterstained with haematoxylin. Sciatic nerve sections were taken from the middle regions of the regenerated nerve in the chamber. After the fixation, the nerve tissue was post-fixed in 0.5 per cent osmium tetroxide, dehydrated and embedded in spurs. The tissue was then cut to 5 μm thickness using a microtome with a dry glass knife, stained with toluidine blue.

2.12. Image analysis

All tissue samples were observed under optical microscopy. CGRP-immunoreactivity (IR) in dorsal horn in the lumbar spinal cord was detected by immunohistochemistry as described previously [29]. The immunoproducts were confirmed to be positive-labelled if their density level was over five times the background levels. Under a 100× magnification, the ratio of area occupied by positive CGRP-IR in dorsal horn ipsilateral to the injury following neurorrhaphy relative to the lumbar spinal cord was measured using an image analyzer system (Image-Pro Lite, Media Cybernetics, USA) coupled to the microscope.

As counting the myelinated axons, at least 30–50% of the sciatic nerve section area randomly selected from each nerve specimen at a magnification of 400× was observed. The axon counts were extrapolated by using the area algorithm to estimate the total number of axons for each nerve. Axon density was then obtained by dividing the axon counts by the total nerve areas. All data are expressed as mean ± standard deviation. Statistical comparisons between groups were made by the one-way analysis of variance.

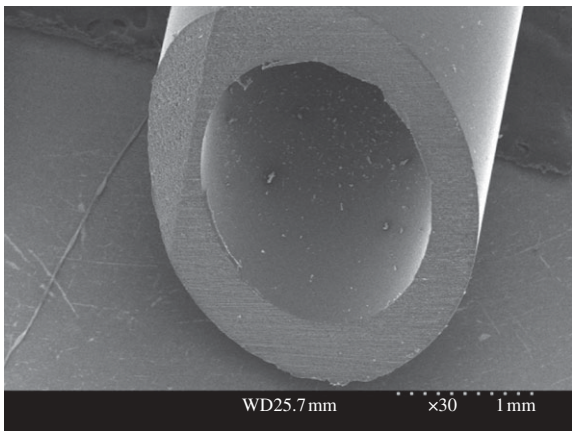

Figure 2. SEM micrograph of the GCC conduit.

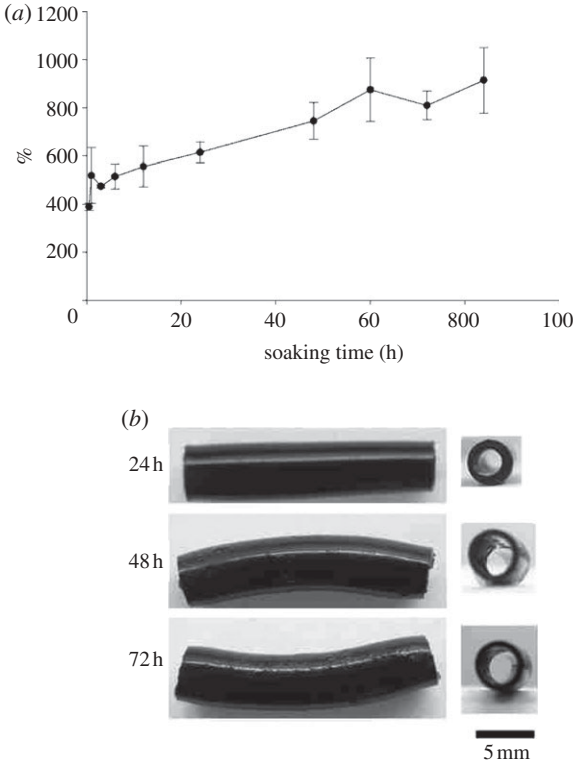

Figure 3. (*a*) Time effect on the water uptake ratio (%) of GCC conduits. (*b*) Macrographs of the GCC conduits soaked in de-ionized water at different periods.

3. RESULTS

3.1. Macroscopic observation of GCC conduits

GCC conduits were dark blue in appearance caused by the reaction between genipin and amino acids or proteins. Figure 2 shows that the GCC conduit was concentric and round with a smooth inner lumen and outer wall surface.

3.2. Physical characteristics of GCC conduits

The cross-linking index of GCC conduits, expressed as a percentage of free amino groups lost during cross-linking, was 13.6 ± 5.2%. This means that 1.0 wt% genipin was sufficient to cross-link about 13.6 per cent of the amino groups. The maximum tensile

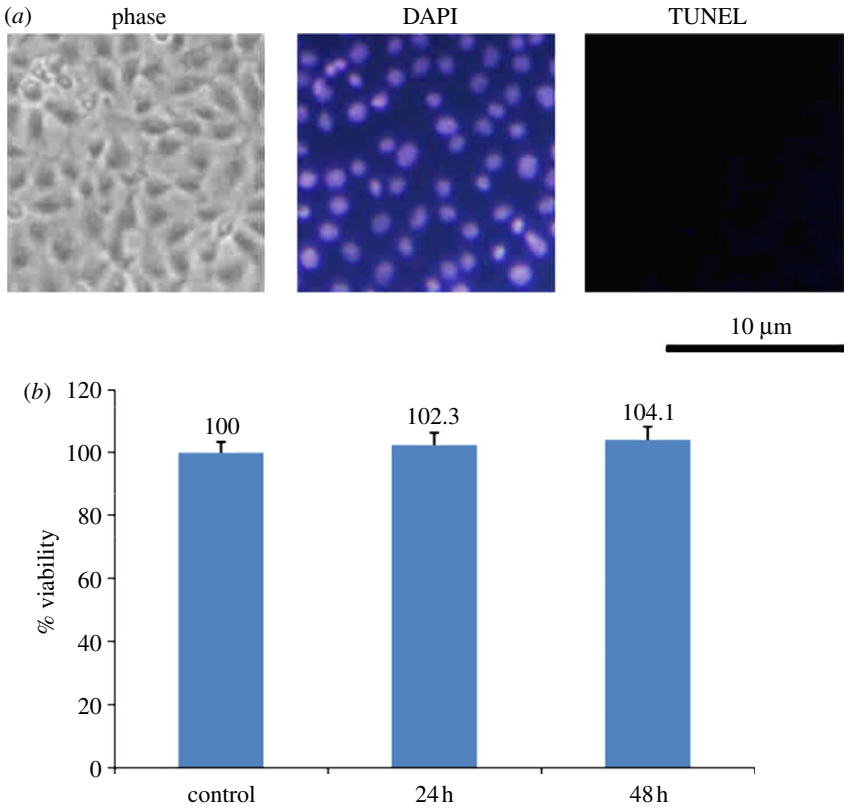

Figure 4. Induction of apoptosis and cytotoxicity by soaking solution of GCC conduits. (*a*) Nuclei of Schwann cells were characterized by DAPI and TUNEL assay and investigated under a fluorescent microscopy. (*b*) Quantification of cytotoxic test of soaking solutions of GCC conduits relative to the controls on Schwann cells. Values are mean ± s.e.

force and the water contact angle of GCC conduits were 165.7 ± 24.9 N and $59.0 \pm 4.5^{\circ}$. These results showed that the GCC conduits could provide enough mechanical strength to resist muscular contraction and their surface was hydrophilic, which was conducive to cell adhesion and growth. Throughout the experimental period, the water uptake ratios of the soaked GCC conduits increased markedly (figure 3*a*). Though the walls of the GCC conduits were swelled as a result of absorption of soaking solution, they still kept their tubular structure without occlusion even after 72 h of soaking (figure 3*b*), indicating that the GCC matrix provided a framework with suitable mechanical strength.

3.3. Cytotoxicity and apoptosis of GCC conduits

The spindle-shaped cellular morphology of Schwann cells cultured on the culture plate was viable and there was no sign of infection. Treatment with the soaking solution of GCC conduits did not induce apoptotic cell death since only very few TUNEL-positive cells were seen, suggesting that DNA fragmentation did not occur in these Schwann cells (figure 4*a*). This result was supported by the cytotoxic test that all GCC scaffolds were considered non-toxic to Schwann cells as cell viability was in the range of 102.3–104.1%, indicated that these GCC scaffolds were suitable for cell culture (figure 4*b*).

3.4. Biocompatibility of GCC conduits

No clinical problems were seen for any of the rats in the post-operative period. The GCC was implanted subcutaneously in the back of the mice and the NF-κB-driven bioluminescent signals were monitored by luminescent imaging on the indicated periods (figure 5*a*). As a result, the luminescent signal in the implanted region was initially increased and dramatically decreased (figure 5*b*). NF-κB activity reached a maximal activation at 3 days where a strong and specific *in vivo* bioluminescence was observed around the implantation site. Consistent with the bioluminescent signals, an acute inflammatory response was observed at the site between GCC conduits and their surrounding tissues even just 1 day post-implantation under optical microscopy, characterized by a rapid accumulation of inflammatory cells (figure 6*a*). Phagocytizing reaction was still obvious at the interfaces between the disintegrated GCC materials and tissues after 3–7 days of implantation (figure 6*b*,*c*). At 28 days, the GCC conduits had been degraded completely (figure 6*d*).

3.5. Electrophysiological measurements

MAPs were recorded at post-operative intervals of two, five and eight weeks. All of the electrophysiological indexes, including amplitude, latency and NCV of the regenerated nerves were improved as a function of the experimental period (figure 7*a*–*c*). Specifically, the difference of the NCV between the nerves at

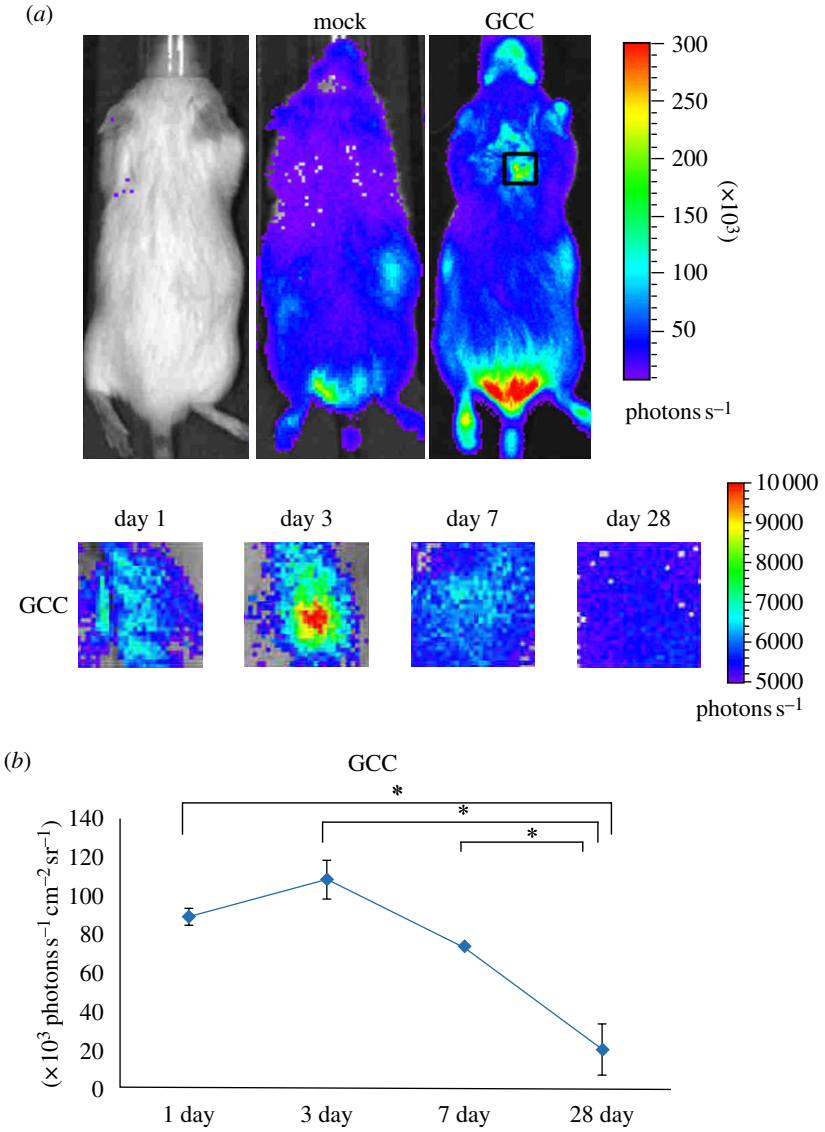

Figure 5. NF-κB-dependent bioluminescence in living mice implanted with GCC conduits. (*a*) Diagrams show the bioluminescent signal within a radius of 2.5 mm of implanted region (boxed area). The colour overlay on the image represents the photons s^{-1} emitted from the animal, as indicated by the colour scales. (*b*) Quantification of photon emission within the implanted region. Values are mean ± s.e. of three mice. $^{*}p < 0.05$, significant difference from other examined time points.

post-operative intervals of two and eight weeks reached the significant level at $p < 0.05$. In addition, the regenerated nerves at eight weeks postoperatively had a significantly shorter latency when compared with those at two and five weeks of recovery ($p < 0.05$). However, the lack of a statistically significant difference in amplitude could imply that the atrophy of the muscle was still serious after eight weeks of recovery, even if muscle fibres had been reinnervated.

3.6. CGRP immunoreactivity in the dorsal horn following injury

Immunohistochemical staining showed that lamina I–II regions in the dorsal horn ipsilateral to the injury were strongly CGRP-immunolabelled at week 2, and then notably decreased from weeks 5 to 8 (figure 8*a*,*b*). CGRP-labelled fibres were also noted in the area of lamina III–V (figure 8*c*). These results indicated that CGRP expression dynamics in the lumbar spinal cord differed depending upon the recovery stage of the regenerating sciatic nerve in the GCC conduit.

3.7. Sciatic nerve regeneration

No nerve dislocation out of the GCC conduits was seen for all of the rats throughout the eight weeks of the experimental period. Brownish fibrous tissue encapsulation was noted covering the GCC conduits (figure 9). After trimming the fibrous tissue, cutting the wall of the tube, the regenerated nerve was exposed and then retrieved. Observing the muscle tissue surrounding the conduit, no obvious inflammation or adhesion was found. Overall gross examination of the GCC conduits at the three observation time points all revealed 100 per cent nerve formation in the tubes.

3.7.1. After two weeks. At two weeks post-implantation, the GCC conduits had been well integrated into the regenerating nerve tissue. Regenerated nerves in the

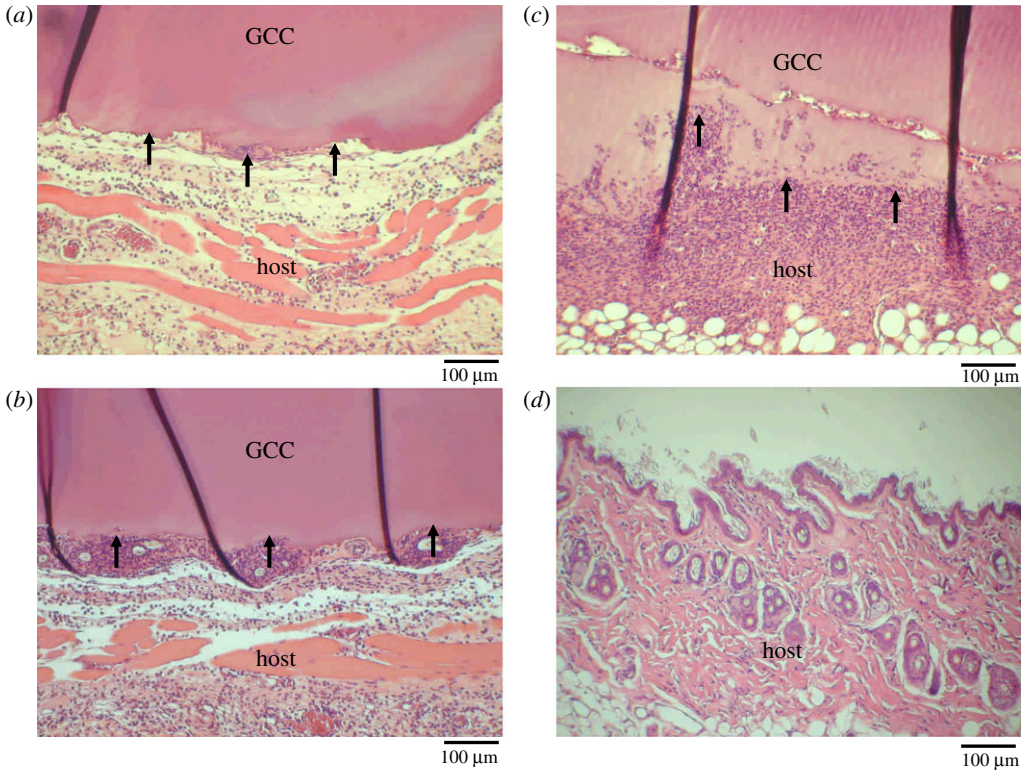

Figure 6. Micrographs of interface area between the host and the GCC conduits implanted for (*a*) 1 day, (*b*) 3 days, (*c*) 7 days and (*d*) 28 days. Note that a rapid accumulation of inflammatory cells phagocytizing the disintegrated GCC materials (black arrows).

GCC conduits were still immature composed of fibrin matrices, which were populated by mast cells and red blood cells (figure 10*a*). This fibrin bridge could provide a framework for subsequent migration of fibroblasts, Schwann cells and axons.

3.7.2. After five weeks. At five weeks, the process of degradation of the GCC conduits was obvious. Only a small amount of wall residues was seen surrounding the regenerating nerve. Up to this time, the regenerated nerves became more mature, displaying a structure with a symmetric and thin epineurium, surrounding a cellular and vascularized endoneurium in which numerous myelinated axons had been seen (figure 10*b*). This area was surrounded by a collagen-rich encapsulating structure in which remnants of the GCC conduit wall and numerous large round cells were observed. It appeared that the GCC conduit was being broken down by these large round cells.

3.7.3. After eight weeks. The GCC conduits had almost totally been degraded, exposing slender regenerated nerves inside. As seen at five weeks of regeneration, the nerves at this stage had a mature structure with a large number of myelinated axons interposed in the endoneurium with rich neovascularization (figure 10*c*). Although maturation of the regenerated nerve tissue progressed with time, an outer encapsulating structure was still noted which contained fragments of GCC and large round cells (figure 10*d*).

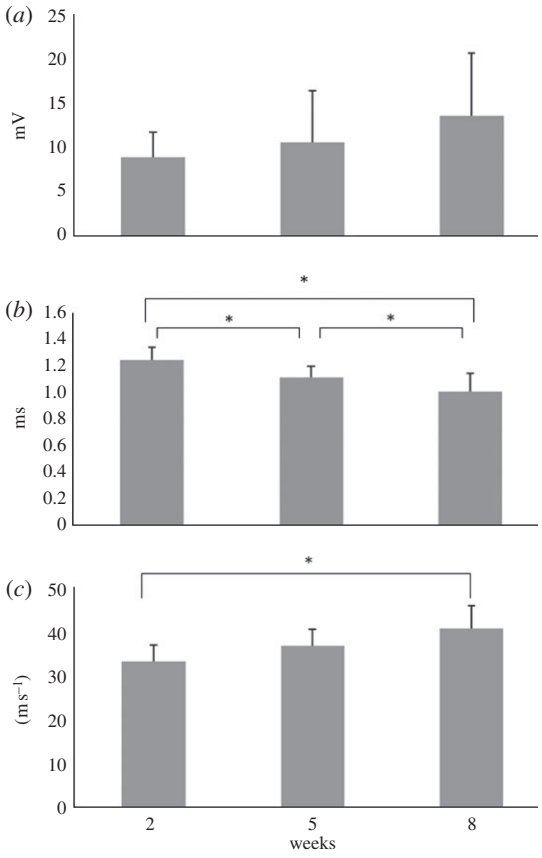

Figure 7. Analysis of the evoked MAPs, including (*a*) peak amplitude, (*b*) latency and (*c*) NCV. $*p < 0.05$, significant difference from other examined time points.

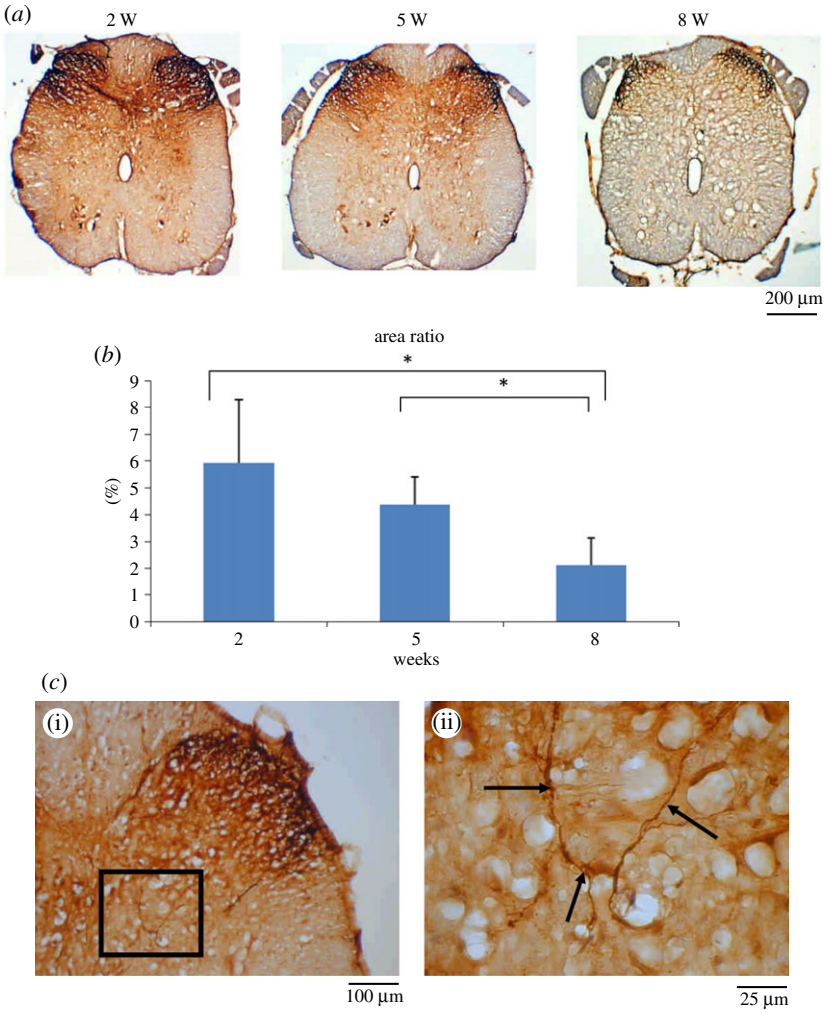

Figure 8. CGRP-IR in dorsal horn in the lumbar spinal cord after injury. (*a*) CGRP-IR was detected by immunohistochemistry, and (*b*) the positive CGRP-IR area ratio was measured. (*c*) Photo shows the area of lamina III–V examined for CGRP-labelled fibres (black arrows). Shown in (*c*(ii)) is the higher magnification of the boxed area in (*c*(i)). $*p < 0.05$, significant difference from other examined time points.

3.8. Morphometric measurements

As aforementioned results, nerve features in the GCC conduits at two weeks of implantation were too immature to be included in the comparisons of their morphometric measurements. By comparison, morphometric studies revealed available data in regenerated nerves in both tube groups after five and eight weeks of implantation for their mean values of myelinated axon number, axon area, axon density and total nerve area (figure 11*a–d*). Especially, it was noted that a significant increase in the axon density and the axon area at the significant level of 0.05 for both the postoperative intervals. In addition, large variations of total nerve area and axon number occurred in the regenerated nerves at five weeks postoperatively, indicating that a relatively immature structure formed at this time point.

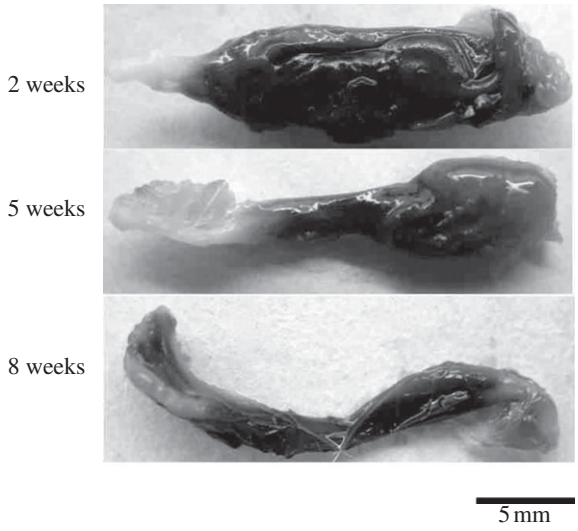

Figure 9. Macrographs of the GCC conduits at different implantation periods.

4. DISCUSSION

For a short nerve injury, the end-to-end and the fascicular suture repair techniques are suggested. However, if the nerve injury is extensive, forming an irreducible gap between the injured proximal and distal stumps, a nerve graft or a nerve bridge is preferred. It is difficult to acquire donor nerves for grafting; therefore, considerable research has been conducted on peripheral

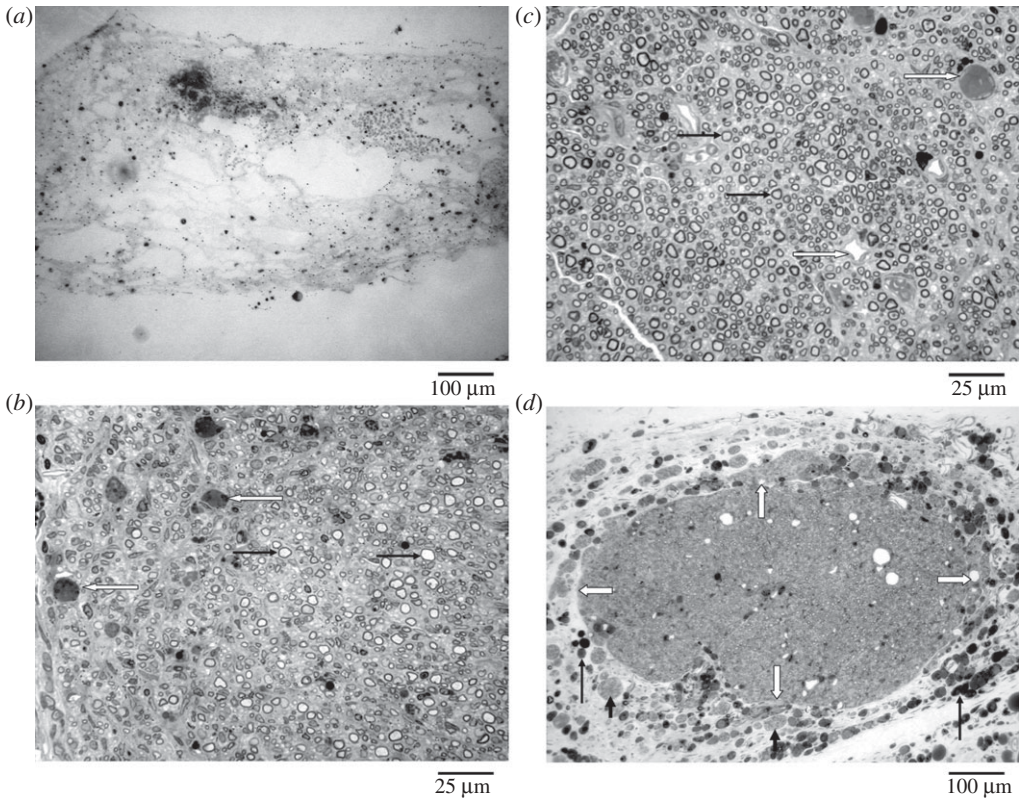

Figure 10. Light micrographs of regenerated nerve cross-sections at different implantation periods: (*a*) 2 weeks, (*b*) 5 weeks and (*c*) 8 weeks. Note a great number of myelinated axons (black arrows) and blood vessels (white arrows) in the nerves after 5 weeks of regeneration. (*d*) An encapsulating structure in which fragments of GCC (long black arrows) and large round cells tissue (short black arrows) were noted surrounding the regenerated nerve (white arrows indicate the border area).

nerve repair using the nerve bridge technique. Most of the successful studies with the nerve bridging model have used a short nerve gap. The inherent regenerative capacity of the nerve in animals could be so efficient over shorter gaps that the benefits of different modifications of the nerve bridging conduit may not be fully revealed. To demonstrate the efficiency of nerve conduits in bridging damaged nerves, a larger gap is therefore suggested.

For improving peripheral nerve regeneration with a large gap, degradable polymer conduits have attracted considerable interest. It is conceivable that different stratagems should be designed for the degradable conduits to assist the growth of regenerating nerves. Ideally, a nerve guide should be composed of a biodegradable material that degrades at a rate in accordance with the rate of axonal elongation during early phases of regeneration. At this stage, the structure of the nerve guides should persist for a sufficient period to allow the formation of a fibrin matrix to connect the proximal and the distal nerve stumps. Once the initial fibrin matrix is formed, the nerve guides should degrade within a reasonable time. Otherwise, delayed nerve regeneration could happen, resulting from the compression by the guide lumen, causing epineural fibrosis thus hampering nerve regeneration and maturation [30].

In this work, a novel protein-based degradable nerve conduit has been prepared and characterized. Naturally occurring genipin was used to cross-link casein, a phosphoprotein that precipitates from raw skim milk by acidification [31]. The affinity of the GCC to the Schwann cells was assessed by cytotoxic testing, TUNEL assay, the contact angle and the water uptake ratio of the materials. As a result, the GCC could maintain the survival and outgrowth of Schwann cells, which had good hydrophilicity and maintained its integrity even after 72 h of soaking in the deionized water. We also constructed transgenic mice carrying the luciferase gene under the control of NF-κB-responsive element to monitor the inflammatory response following implantation of the GCC. Both the non-invasive real-time NF-κB bioluminescence imaging accompanied by the histochemical assessment showed that the GCC was highly biocompatible, only evoking a mild tissue response. These results are not surprising as the casein has been shown to be a promising material for use in pharmaceutical applications [32,33], and the genipin shows prominent neuritogenic activity in paraneurons such as PC12h cells [34,35].

From *in vivo* observations, we found that the cellular activity within the GCC conduits appeared to be a promising medicinal product for repair of peripheral nerve defects. We can see that the GCC conduits degraded as a function of the implantation period. However, they still kept their functional capability as a structural cuff even after eight weeks of implantation. As the luminal adequacy is paramount in determining the extent of nerve regeneration, we believe that the stable dimensions of the GCC conduits played a critical

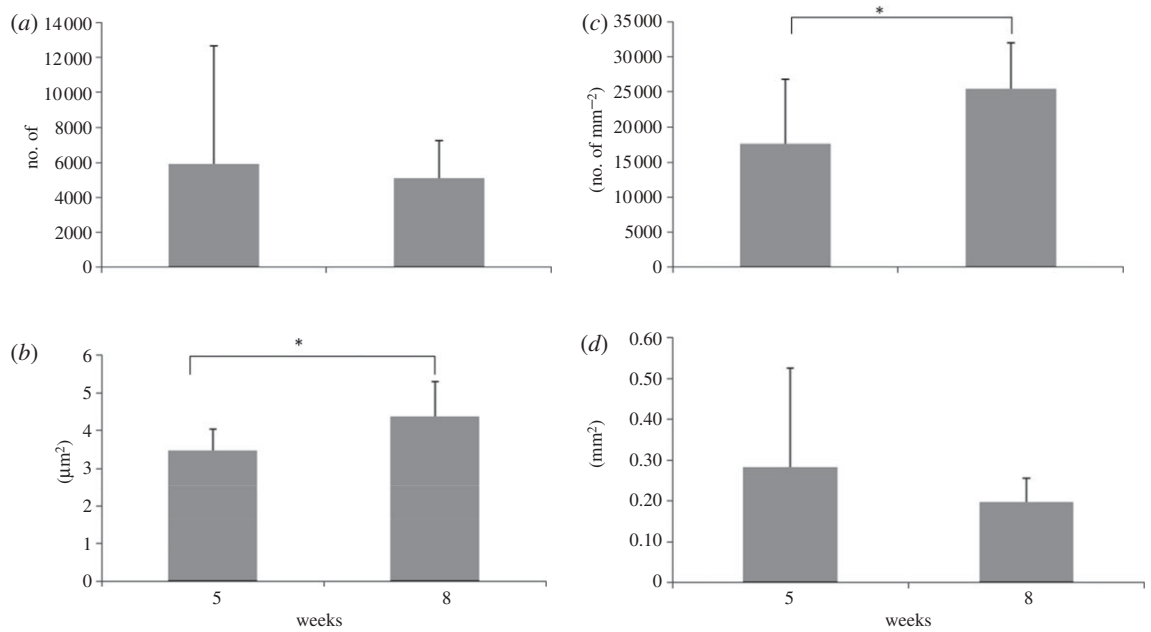

Figure 11. Morphometric analysis from the regenerated nerves in the GCC conduits, including (*a*) axon number, (*b*) axon area, (*c*) axon density and (*d*) total nerve area. $*p < 0.05$, significant difference from other examined time points.

Table 1. Experimental details of recent studies on biodegradable bridging conduits to repair injured rat sciatic nerves.

reference	cuff materials	gap (mm)	myelinated axons	findings
[41]	genipin cross-linked gelatin (GGT) annexed with β-tricalcium phosphate ceramic particles	10	six weeks, midpoint 2523 ± 286	newly formed nerve fibres in the GGT conduits exceed that of the silicone tubes (1195 ± 183) during the implantation period
[17]	chitosan	10	12 weeks, midpoint 15 300 (axon mm^{-2})	chitosan is a potential material to nerve grafting
[2]	polylactic acid (PLA)	10	eight weeks, midpoint mostly unmyelinated axons	multi-layer microbraided PLA fibre-reinforced conduits provide a promising tool for neuroregeneration
[30]	porous genipin cross-linked gelatine (PGGC)	10	eight weeks, midpoint 4000	PGGCs can not only offer effective aids for regenerating nerves but also accelerate favourable nerve-functional recovery when compared with non-porous genipin cross-linked gelatine conduits
[42]	chitosan–polylactic acid (PLA)	10	12 weeks, distal 6275 ± 2000	axonal quantity of chitosan–PLA tubes are higher than silicone rubber tubes (2648 ± 685)
[43]	proanthocyanidin (PA) cross-linked gelatine	10	eight weeks, midpoint mostly unmyelinated axons	the peak amplitude, area under the MAP curve, and the histological observations of regenerated nerves all increase with the recovery period
[7]	polyglycolic acid (PGA)	10	15 weeks, distal 189 ± 55 (axon/ 100×100 μm^2)	type I collagen conduit is a reliable alternative to nerve grafting for gaps up to 10 mm in length
	type I collagen	10	15 weeks, distal 381 ± 73 (axon/ 100×100 μm^2)	
[22]	genipin cross-linked gelatin	10	eight weeks, midpoint mostly unmyelinated axons ($n = 10$)	histological observations show that numerous regenerated nerve fibres, mostly unmyelinated and surrounded by Schwann cells, cross through and beyond the gap region six weeks after operation

role in the high success of nerve regeneration in the present study. Therefore, the GCC can be considered as an ideal tubulization material as it can provide a suitable and continuous support to protect the regenerating axons from invasion by the surrounding connective tissue. The stable dimensions of the GCC conduits could result from the chemical cross-linking of genipin with the amino groups on the casein macromolecular chains [36]. After completion of their guiding function, the GCC conduits degraded and were well integrated with the regenerating nerve tissues. At two weeks of regeneration, regenerated nerve cables were composed of fibrin matrices which were populated by mast cells and red blood cells. After five weeks of recovery, the regenerated nerves were well vascularized and myelinated axons were numerous in their endoneurial areas, which were surrounded by a collagen-rich encapsulating structure. The encapsulation tissue is commonly seen as using a biodegradable conduit for nerve regeneration, which comes from the cellular activity during the process of degradation of the nerve guide that evokes neural fibrosis [37]. These histological results were supported by the protein levels of CGRP in the associated spinal cord segments, which were gradually decreased during the test period. Since the CGRP has been recognized as a nerve regeneration-promoting peptide *in vivo* [38–40], it is conceivable that the declining CGRP expression in the spines may be attributable to the fact that, nerves at their late stage of regeneration in the GCC conduits were more mature; thus, injury-related signals derived from these nerves which could be retrogradely transported to neurons in the dorsal horn and subsequently trigger these cells to synthesize and release CGRP became less. Morphometric studies also indicated that the recovery of the regenerated nerves was progressing as a function of the experimental period, which suggested that the transected nerve had undergone adequate regeneration in the GCC conduits. The experimental test details, used in several recent studies on biodegradable bridging conduits to repair injured rat sciatic nerves, were gleaned from the literature and summarized (table 1). It is noted that the regenerated nerves in the GCC conduits are more mature with larger mean values of myelinated axon count (approx. 6000) and axonal density (approx. 25 000 mm^{-2}) than those in the conduits made of various biodegradable materials reported in the literature, such as the chitosan [17], the PLA [2], the PGA [7], the proanthocyanidin (PA) cross-linked gelatine [43] and the genipin cross-linked gelatine (GGT) [22,30]. In addition, the temporal and spatial progresses of cellular activity within the GCC conduit are better than those seen for experiments using silicone rubber nerve guides [41,42], which have largely been used in clinical practice. These results again show the advantages of the GCC conduits, which could promote the regeneration and maturity of injured nerves.

5. CONCLUSION

The current study is the first work dedicated to GCC conduits, a newly devised natural nerve bridge. Such nerve guides seem to be promising candidates to be applied as an alternative material for the clinical repair of large peripheral nerve defects as they are well-integrated into the host tissue with a mild foreign body reaction and support myelinated axonal regeneration and functional recovery.

The authors would like to thank China Medical University (Contract No. CMU99-S-43), National Science Council of the Republic of China, Taiwan (Contract No. NSC99-2221-E-039-006-MY3) and Taiwan Department of Health Clinical Trial and Research Center of Excellence (Contract No. DOH100-TD-B-111-004) for financially supporting this research.

REFERENCES

1 Ateh, D. D., Navsaria, H. A. & Vadgama, P. 2006 Polypyrrole-based conducting polymers and interactions with biological tissues. *J. R. Soc. Interface* **3**, 741–752. (doi:10.1098/rsif.2006.0141)
2 Lu, M. C., Huang, Y. T., Lin, J. H., Yao, C. H., Lou, C. W., Tsai, C. C. & Chen, Y. S. 2009 Evaluation of a multi-layer microbraided polylactic acid fiber-reinforced conduit for peripheral nerve regeneration. *J. Mater. Sci. Mater. Med.* **20**, 1175–1180. (doi:10.1007/s10856-008-3646-4)
3 Wang, H. B., Mullins, M. E., Cregg, J. M., Hurtado, A., Oudega, M., Trombley, M. T. & Gilbert, R. J. 2009 Creation of highly aligned electrospun poly-L-lactic acid fibers for nerve regeneration applications. *J. Neural Eng.* **6**, 016001. (doi:10.1088/1741-2560/6/1/016001)
4 Wang, H. B., Mullins, M. E., Cregg, J. M., McCarthy, C. W. & Gilbert, R. J. 2010 Varying the diameter of aligned electrospun fibers alters neurite outgrowth and Schwann cell migration. *Acta Biomater.* **6**, 2970–2978. (doi:10.1016/j.actbio.2010.02.020)
5 Hu, W., Gu, J., Deng, A. & Gu, X. 2008 Polyglycolic acid filaments guide Schwann cell migration *in vitro* and *in vivo*. *Biotechnol. Lett.* **30**, 1937–1942. (doi:10.1007/s10529-008-9795-1)
6 Huang, J. H., Cullen, D. K., Browne, K. D., Groff, R., Zhang, J., Pfister, B. J., Zager, E. L. & Smith, D. H. 2009 Long-term survival and integration of transplanted engineered nervous tissue constructs promotes peripheral nerve regeneration. *Tissue Eng. Part A* **15**, 1677–1685. (doi:10.1089/ten.tea.2008.0294)
7 Waitayawinyu, T., Parisi, D. M., Miller, B., Luria, S., Morton, H. J., Chin, S. H. & Trumble, T. E. 2007 A comparison of polyglycolic acid versus type 1 collagen bioabsorbable nerve conduits in a rat model: an alternative to autografting. *J. Hand Surg. Am.* **32**, 1521–1529. (doi:10.1016/j.jhsa.2007.07.015)
8 Mano, J. F. *et al.* 2007 Natural origin biodegradable systems in tissue engineering and regenerative medicine: present status and some moving trends. *J. R. Soc. Interface* **4**, 999–1030. (doi:10.1098/rsif.2007.0220)
9 Madduri, S., Feldman, K., Tervoort, T., Papaloïzos, M. & Gander, B. 2010 Collagen nerve conduits releasing the neurotrophic factors GDNF and NGF. *J. Control. Rel.* **143**, 168–174. (doi:10.1016/j.jconrel.2009.12.017)
10 Pereira Lopes, F. R., Frattini, F., Marques, S. A., Almeida, F. M., de Moura Campos, L. C., Langone, F., Lora, S., Borojevic, R. & Martinez, A. M. 2010 Transplantation of bone-marrow-derived cells into a nerve guide resulted in transdifferentiation into Schwann cells and effective regeneration of transected mouse sciatic nerve. *Micron* **41**, 783–790. (doi:10.1016/j.micron.2010.05.010)

11 Yao, L., de Ruiter, G. C., Wang, H., Knight, A. M., Spinner, R. J., Yaszemski, M. J., Windebank, A. J. & Pandit, A. 2010 Controlling dispersion of axonal regeneration using a multichannel collagen nerve conduit. *Biomaterials* **31**, 5789–5797. (doi:10.1016/j.biomaterials.2010.03.081)

12 Alvarez-Perez, M. A., Guarino, V., Cirillo, V. & Ambrosio, L. 2010 Influence of gelatin cues in PCL electrospun membranes on nerve outgrowth. *Biomacromolecules* **11**, 2238–2246. (doi:10.1021/bm100221h)

13 Ghasemi-Mobarakeh, L., Prabhakaran, M. P., Morshed, M., Nasr-Esfahani, M. H. & Ramakrishna, S. 2008 Electrospun poly(epsilon-caprolactone)/gelatin nanofibrous scaffolds for nerve tissue engineering. *Biomaterials* **29**, 4532–4539. (doi:10.1016/j.biomaterials.2008.08.007)

14 Wang, L. S., Chung, J. E., Chan, P. P. & Kurisawa, M. 2010 Injectable biodegradable hydrogels with tunable mechanical properties for the stimulation of neurogenesic differentiation of human mesenchymal stem cells in 3D culture. *Biomaterials* **31**, 1148–1157. (doi:10.1016/j.biomaterials.2009.10.042)

15 Li, X., Wang, W., Wei, G., Wang, G., Zhang, W. & Ma, X. 2010 Immunophilin FK506 loaded in chitosan guide promotes peripheral nerve regeneration. *Biotechnol. Lett.* **32**, 1333–1337. (doi:10.1007/s10529-010-0287-8)

16 Shen, H., Shen, Z. L., Zhang, P. H., Chen, N. L., Wang, Y. C., Zhang, Z. F. & Jin, Y. Q. 2010 Ciliary neurotrophic factor-coated polylactic–polyglycolic acid chitosan nerve conduit promotes peripheral nerve regeneration in canine tibial nerve defect repair. *J. Biomed. Mater. Res. B Appl. Biomater.* **95**, 161–170. (doi:10.1002/jbm.b.31696)

17 Wang, G., Lu, G., Ao, Q., Gong, Y. & Zhang, X. 2010 Preparation of cross-linked carboxymethyl chitosan for repairing sciatic nerve injury in rats. *Biotechnol. Lett.* **32**, 59–66. (doi:10.1007/s10529-009-0123-1)

18 Yu, L. M., Miller, F. D. & Shoichet, M. S. 2010 The use of immobilized neurotrophins to support neuron survival and guide nerve fiber growth in compartmentalized chambers. *Biomaterials* **31**, 6987–6999. (doi:10.1016/j.biomaterials.2010.05.070)

19 Aimutis, W. R., Kornegay, E. T. & Eigel, W. N. 1982 Electrophoretic and biochemical comparison of casein and whey protein from porcine colostrum and milk. *J. Dairy Sci.* **65**, 1874–1881. (doi:10.3168/jds.S0022-0302(82)82432-6)

20 Eigel, W. N., Hofmann, C. J., Chibber, B. A., Tomich, J. M., Keenan, T. W. & Mertz, E. T. 1979 Plasmin-mediated proteolysis of casein in bovine milk. *Proc. Natl Acad. Sci. USA* **76**, 2244–2248. (doi:10.1073/pnas.76.12.2244)

21 Bispo, V. M., Mansur, A. A., Barbosa-Stancioli, E. F. & Mansur, H. S. 2010 Biocompatibility of nanostructured chitosan/poly(vinyl alcohol) blends chemically crosslinked with genipin for biomedical applications. *J. Biomed. Nanotechnol.* **6**, 166–175. (doi:10.1166/jbn.2010.1110)

22 Chen, Y. S., Chang, J. Y., Cheng, C. Y., Tsai, F. J., Yao, C. H. & Liu, B. S. 2005 An *in vivo* evaluation of a biodegradable genipin-cross-linked gelatin peripheral nerve guide conduit material. *Biomaterials* **26**, 3911–3918. (doi:10.1016/j.biomaterials.2004.09.060)

23 Harris, R., Lecumberri, E. & Heras, A. 2010 Chitosan-genipin microspheres for the controlled release of drugs: clarithromycin, tramadol and heparin. *Mar. Drugs* **8**, 1750–1762. (doi:10.3390/md8061750)

24 Chi, G. F., Kim, M. R., Kim, D. W., Jiang, M. H. & Son, Y. 2010 Schwann cells differentiated from spheroid-forming cells of rat subcutaneous fat tissue myelinate axons in the spinal cord injury. *Exp. Neurol.* **222**, 304–317. (doi:10.1016/j.expneurol.2010.01.008)

25 Liu, H., Kim, Y., Chattopadhyay, S., Shubayev, I., Dolkas, J. & Shubayev, V. I. 2010 Matrix metalloproteinase inhibition enhances the rate of nerve regeneration *in vivo* by promoting dedifferentiation and mitosis of supporting Schwann cells. *J. Neuropathol. Exp. Neurol.* **69**, 386–395. (doi:10.1097/NEN.0b013e3181d68d12)

26 Wang, J., Zhang, P., Wang, Y., Kou, Y., Zhang, H. & Jiang, B. 2010 The observation of phenotypic changes of Schwann cells after rat sciatic nerve injury. *Artif. Cells Blood Substit. Immobil. Biotechnol.* **38**, 24–28. (doi:10.3109/10731190903495736)

27 Ho, T. Y., Chen, Y. S. & Hsiang, C. Y. 2007 Noninvasive nuclear factor-kappaB bioluminescence imaging for the assessment of host–biomaterial interaction in transgenic mice. *Biomaterials* **28**, 4370–4377. (doi:10.1016/j.biomaterials.2007.07.005)

28 Hsiang, C. Y., Chen, Y. S. & Ho, T. Y. 2009 Nuclear factor-kappaB bioluminescence imaging-guided transcriptomic analysis for the assessment of host–biomaterial interaction *in vivo*. *Biomaterials* **30**, 3042–3049. (doi:10.1016/j.biomaterials.2009.02.016)

29 Zheng, L. F., Wang, R., Xu, Y. Z., Yi, X. N., Zhang, J. W. & Zeng, Z. C. 2008 Calcitonin gene-related peptide dynamics in rat dorsal root ganglia and spinal cord following different sciatic nerve injuries. *Brain Res.* **1187**, 20–32. (doi:10.1016/j.brainres.2007.10.044)

30 Chang, J. Y., Ho, T. Y., Lee, H. C., Lai, Y. L., Lu, M. C., Yao, C. H. & Chen, Y. S. 2009 Highly permeable genipin-cross-linked gelatin conduits enhance peripheral nerve regeneration. *Artif. Organs* **33**, 1075–1085. (doi:10.1111/j.1525-1594.2009.00818.x)

31 Bansal, N., Fox, P. F. & McSweeney, P. L. 2007 Factors affecting the retention of rennet in cheese curd. *J. Agric. Food Chem.* **55**, 9219–9225. (doi:10.1021/jf071105p)

32 Song, F., Zhang, L. M., Shi, J. F. & Li, N. N. 2010 Novel casein hydrogels: formation, structure and controlled drug release. *Colloids Surf. B. Biointerfaces* **79**, 142–148. (doi:10.1016/j.colsurfb.2010.03.045)

33 Trejo, R. & Harte, F. 2010 The effect of ethanol and heat on the functional hydrophobicity of casein micelles. *J. Dairy Sci.* **93**, 2338–2343. (doi:10.3168/jds.2009-2918)

34 Yamazaki, M., Chiba, K. & Mohri, T. 2006 Differences in neuritogenic response to nitric oxide in PC12 and PC12h cells. *Neurosci. Lett.* **393**, 222–225. (doi:10.1016/j.neulet.2005.09.068)

35 Yamazaki, M., Chiba, K., Mohri, T. & Hatanaka, H. 2004 Cyclic GMP-dependent neurite outgrowth by genipin and nerve growth factor in PC12h cells. *Eur. J. Pharmacol.* **488**, 35–43. (doi:10.1016/j.ejphar.2004.02.009)

36 Song, F., Zhang, L. M., Yang, C. & Yan, L. 2009 Genipin-crosslinked casein hydrogels for controlled drug delivery. *Int. J. Pharm.* **373**, 41–47. (doi:10.1016/j.ijpharm.2009.02.005)

37 Den Dunnen, W. F. A., Van Der Lei, B., Schakenraad, J. M., Blaauw, E. H., Stokroos, I., Pennings, A. J. & Robinson, P. H. 1993 Long-term evaluation of nerve regeneration in a biodegradable nerve guide. *Microsurgery* **14**, 508–515. (doi:10.1002/micr.1920140808)

38 Belyantseva, I. A. & Lewin, G. R. 1999 Stability and plasticity of primary afferent projections following nerve regeneration and central degeneration. *Eur. J. Neurosci.* **11**, 457–468. (doi:10.1046/j.1460-9568.1999.00458.x)

39 Blesch, A. & Tuszynski, M. H. 2001 GDNF gene delivery to injured adult CNS motor neurons promotes axonal growth, expression of the trophic neuropeptide CGRP, and cellular protection. *J. Comp. Neurol.* **436**, 399–410. (doi:10.1002/cne.1076)

40 Chen, L. J., Zhang, F. G., Li, J., Song, H. X., Zhou, L. B., Yao, B. C., Li, F. & Li, W. C. 2010 Expression of calcitonin gene-related peptide in anterior and posterior horns of the spinal cord after brachial plexus injury. *J. Clin. Neurosci.* **17**, 87–91. (doi:10.1016/j.jocn.2009.03.042)

41 Yang, Y. C., Shen, C. C., Huang, T. B., Chang, S. H., Cheng, H. C. & Liu, B. S. 2010 Characteristics and biocompatibility of a biodegradable genipin-cross-linked gelatin/β-tricalcium phosphate reinforced nerve guide conduit. *J. Biomed. Mater. Res. B Appl. Biomater.* **95**, 207–217. (doi:10.1002/jbm.b.31705)

42 Xie, F., Li, Q. F., Gu, B., Liu, K. & Shen, G. X. 2008 *In vitro* and *in vivo* evaluation of a biodegradable chitosan-PLA composite peripheral nerve guide conduit material. *Microsurgery* **28**, 471–479. (doi:10.1002/micr.20514)

43 Liu, B. S. 2008 Fabrication and evaluation of a biodegradable proanthocyanidin-crosslinked gelatin conduit in peripheral nerve repair. *J. Biomed. Mater. Res. A* **87**, 1092–1102. (doi:10.1002/jbm.a.31916)